Science of the Total Environment 461–462 (2013) 39–48

Contents lists available at SciVerse ScienceDirect

Science of the Total Environment

journal homepage: www.elsevier.com/locate/scitotenv

Light-induced catalytic transformation of ofloxacin by solar Fenton in various water matrices at a pilot plant: Mineralization and characterization of major intermediate products

I. Michael [a], E. Hapeshi [a], J. Aceña [b], S. Perez [b], M. Petrović [b,d], A. Zapata [c], D. Barceló [b,d], S. Malato [c], D. Fatta-Kassinos [a,*]

[a] NIREAS, International Water Research Centre, University of Cyprus, Kallipoleos 75, P.O. Box 20537, 1678 Nicosia, Cyprus
[b] Department of Environmental Chemistry, IDAEA-CSIC, c/JordiGirona 18-26, 08034 Barcelona, Spain
[c] Plataforma Solar de Almería (CIEMAT), Carretera Senéskm 4, 04200 Tabernas (Almería), Spain
[d] Catalan Institute of Water Research, c/Emili Grahit, 101, Edifici H2O, Parc Científic I Tecnològic de la Universitat de Girona, Girona 17003, Spain

HIGHLIGHTS

- The pilot-scale solar Fenton degradation of ofloxacin was studied.
- Mineralization was lower in the wastewater matrices due to the presence of organics.
- Toxicity was found to originate from the oxidation of DOM present in the RE.
- The transformation of OFX proceeded through the formation of seven intermediates.
- The degradation pathway exhibited differences among the four matrices.

GRAPHICAL ABSTRACT

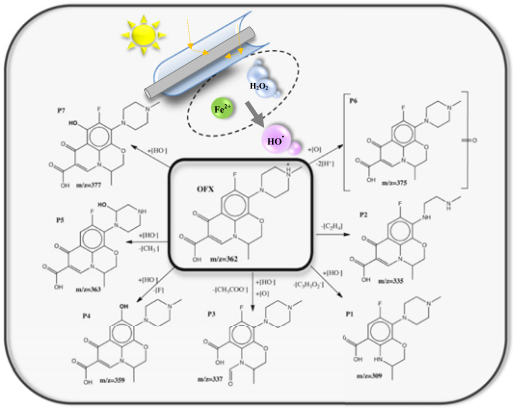

ARTICLE INFO

Article history:
Received 6 February 2013
Received in revised form 5 April 2013
Accepted 18 April 2013
Available online 25 May 2013

Editor: Adrian Covaci

ABSTRACT

This work investigated the application of a solar driven advanced oxidation process (solar Fenton), for the degradation of the antibiotic ofloxacin (OFX) in various environmental matrices at a pilot-scale. All experiments were carried out in a compound parabolic collector pilot plant in the presence of doses of H_2O_2 (2.5 mg L^{-1}) and at an initial Fe^{2+} concentration of 2 mg L^{-1}. The water matrices used for the solar Fenton experiments were: demineralized water (DW), simulated natural freshwater (SW), simulated effluent from municipal wastewater treatment plant (SWW) and pre-treated real effluent from municipal wastewater treatment plant (RE) to which OFX had been spiked at 10 mg L^{-1}. Dissolved organic carbon removal was

Abbreviations: AOPs, Advanced oxidation processes; CPCs, Compound parabolic collectors; DOC, Dissolved organic carbon; DOM, Dissolved organic matter; DW, Demineralized water; FQs, Fluoroquinolones; HPLC-DAD, High performance liquid chromatography with diode array detector; LC–ToF-MS, Liquid chromatography–time of flight-mass spectrometry; MWTP, Municipal wastewater treatment plant; NDIR, Non-dispersive infrared detector; OFX, Ofloxacin; RE, Pre-treated real effluent from municipal wastewater treatment plant; SW, Simulated natural freshwater; SWW, Simulated effluent from municipal wastewater treatment plant; TOC, Total organic carbon; TPs, Transformation products.

* Corresponding author. Tel.: +357 22893515; fax: +357 22895080.
E-mail address: dfatta@ucy.ac.cy (D. Fatta-Kassinos).

http://dx.doi.org/10.1016/j.scitotenv.2013.04.054

Keywords:
Antibiotics
Ofloxacin
QToF-MS
Solar Fenton
Transformation products

found to be dependent on the chemical composition of the water matrix. OFX mineralization was higher in DW (78.1%) than in SW (58.3%) at 12 mg L^{-1} of H_2O_2 consumption, implying the complexation of iron or the scavenging of hydroxyl radicals by the inorganic ions present in SW. On the other hand, the presence of dissolved organic matter (DOM) in SWW and RE, led to lower mineralization per dose of H_2O_2 compared to DW and SW. The major transformation products (TPs) formed during the solar Fenton treatment of OFX, were elucidated using liquid chromatography–time of flight-mass spectrometry (LC–ToF-MS). The transformation of OFX proceeded through a defluorination reaction, accompanied by some degree of piperazine and quinolone substituent transformation while a hydroxylation mechanism occurred by attack of the hydroxyl radicals generated during the process leading to the formation of TPs in all the water matrices, seven of which were tentatively identified. The results obtained from the toxicity bioassays indicated that the toxicity originates from the DOM present in RE and its oxidation products formed during the photocatalytic treatment and not from the TPs resulted from the oxidation of OFX.

1. Introduction

Antibiotics have been detected in various compartments of the aquatic environment worldwide (Fatta-Kassinos et al., 2011; Jeong et al., 2010). This indicates the ineffectiveness of the currently most frequently applied conventional biological treatment processes to remove such compounds adequately from the domestic wastewaters (Michael et al., 2013). Looking into the transformation of the antibiotics in the environment is very important for understanding the fate and behavior of these compounds. The presence of antibiotics and their transformation products (TPs) in low concentrations has been associated to chronic toxicity and the prevalence of resistance to antibiotics in bacterial species (Le-Minh et al., 2010). The consequences are particularly worrying in aquatic organisms as these are subjected to multigenerational exposure (Rosal et al., 2010). Although antibiotics are found in the environment at sub-inhibitory levels, relatively low concentrations of them can still promote bacterial resistance (Castiglioni et al., 2008). Indeed, antibiotic-resistant bacteria have been detected in wastewater effluents (Guardabassi et al., 2002; Akiyama and Savin, 2010; Novo and Manaia, 2010), surface water (Ash et al., 2002) and drinking water (Schwartz et al., 2003).

Fluoroquinolones (FQs) are broad-spectrum antibacterial agents widely used for treating bacterial infections (Paul et al., 2007). Their major mode of action is the inhibition of DNA replication in bacteria via interference of the normal function of DNA topoisomerase (Lhiaubet-Vallet et al., 2009). Although conventional activated sludge treatment can remove a significant fraction of FQs primarily by adsorption to sludge, their removal is incomplete, and FQs are discharged in treated wastewater (Paul et al., 2010). A representative example is ofloxacin (OFX) that has been frequently detected in various environmental compartments (Miao et al., 2004; Lin et al, 2009; Fatta-Kassinos et al., 2010; Zuccato et al., 2010). Regarding its environmental effects, Kümmerer et al. (2000) have found OFX to be genotoxic at environmentally-relevant concentrations while its phototransformation products were found to induce genotoxic effects (Vasquez et al., 2012). OFX was also categorized as posing a high hazard in the aquatic system due to the reuse of biosolids on agriculture land (Langdon et al., 2010).

Promising technologies for the treatment of non-biodegradable and/or toxic compounds are the advanced oxidation processes (AOPs), involving the in situ production of hydroxyl radicals (HO•HO•). Photo-Fenton has gained increasing attention due to its environmentally friendly application and the prospect of operating under solar irradiation hence, lowering the operation cost considerably (Malato et al., 2009; Mendez-Arriaga et al., 2010). The Fenton process consists of the use of ferrous iron salts and hydrogen peroxide in acidic medium. The combination of both reagents (in the presence of UV–vis irradiation) has a very strong synergetic effect because irradiation with light up to 580 nm leads to photoreduction of dissolved ferric iron to ferrous iron producing additional hydroxyl radicals. The mechanism, via which this process mainly occurs, has been comprehensively presented in the literature (Buda et al., 2001; Malato et al., 2009).

In a previous study, the pilot-scale solar degradation of trimethoprim in different water matrices was investigated (Michael et al., 2012), while the current work entailed the investigation of OFX during solar Fenton treatment at a pilot scale. OFX was selected in the present study due to its high photoactivity, its high consumption and presence in wastewater effluents and the aquatic environment. The degradation of OFX induced by various AOPs at a bench scale has been investigated under different experimental conditions: photocatalysis in the presence of TiO_2 (Calza et al., 2008; Michael et al., 2010; Vasquez et al., 2012), solar Fenton (Michael et al., 2010), sonophotocatalysis (Hapeshi et al., in press), photolysis (Wammer et al., 2012) and γ-radiolysis (Santoke et al., 2009). The photocatalytic transformation mechanisms of OFX during solar Fenton oxidation have not been published yet, even if studies relating to its environmental risks are reported in the literature (Albini and Monti, 2003; Park et al., 2002).

With this aim in mind, attention was paid to: (i) determining the effect of the composition of various aqueous matrices on the mineralization; (ii) elucidating the major transformation products (TPs) formed during the solar Fenton treatment of OFX; and (iii) assessing the acute toxicity of OFX and its oxidation products as a whole mixture generated during the treatment process. According to the authors' knowledge the current work, although its general methodology has been presented in various other publications (Klamerth et al., 2009, 2010; Sirtori et al., 2010), is the first one revealing data regarding the pilot-scale solar Fenton oxidation of OFX in four water matrices of different compositions, the elucidation of the main TPs and finally the acute toxicity of OFX and its TPs.

2. Materials and methods

2.1. Chemicals

High purity (>98.5%) OFX standard (CAS number 82419-36-1) was purchased from Sigma-Aldrich. The reagents used in the solar Fenton experiments were iron sulfate heptahydrate ($FeSO_4 \cdot 7H_2O$) and hydrogen peroxide (H_2O_2 30%, w/w) both provided by Panreac. The pH of the matrix under investigation was adjusted (around 2.8–2.9) by 2 N H_2SO_4 supplied by Panreac. The treated solutions were neutralized by 2 N NaOH (Panreac) for toxicity analyses. HPLC-grade acetonitrile (Panreac) and formic acid (Fluka) were used for the chromatographic analysis. Calcium sulfate dehydrate ($CaSO_4 \cdot 2H_2O$, Panreac), magnesium sulfate ($MgSO_4$, Sigma-Aldrich) and potassium chloride (KCl, J.T. Baker) were used for the simulated natural freshwater (SW) preparation. Peptone (Biolife), meat extract (Biolife), urea (Fluka), magnesium sulfate heptahydrate ($MgSO_4 \cdot 7H_2O$, Fluka), dipotassium phosphate (K_2HPO_4, Riedel-de Haën), calcium chloride

dehydrate ($CaCl_2 \cdot 2H_2O$, Riedel-de Haën) and sodium chloride (NaCl, Merck) were the main ingredients for the simulated wastewater (SWW) preparation.

2.2. Water matrices

The water matrices used for the solar Fenton experiments were: demineralized water (DW), simulated natural freshwater (SW), simulated municipal wastewater (SWW) and pre-treated real effluent from secondary treatment (activated sludge) from municipal wastewater treatment plant (RE) to which OFX had been spiked at 10 mg L^{-1}. DW used in the pilot plant was supplied by the Plataforma Solar de Almería (PSA) distillation plant (conductivity < 10 μS cm^{-1}, Cl^- = 0.7–0.8 mg L^{-1}, NO_3^- < 0.5 mg L^{-1}, organic carbon < 1.5 mg L^{-1}). SW and SWW were prepared according to APHA Standard Methods (Clesceri et al., 1998). SW was standard moderately-hard freshwater that was prepared by mixing 60 mg L^{-1} of $CaSO_4 \cdot 2H_2O$, 60 mg L^{-1} of $MgSO_4$ and 4 mg L^{-1} of KCl. Although SW recipe includes bicarbonates (96 mg L^{-1} $NaHCO_3$), it was decided to avoid this addition because based on previous experiments it is proved that under acidic conditions, the carbonate species cannot exist in solution as they are converted into CO_2.

The SWW was prepared by mixing SW and various compounds such as: 32 mg L^{-1} peptone, 22 mg L^{-1} meat extract, 6 mg L^{-1} urea, 2 mg L^{-1} $MgSO_4 \cdot 7H_2O$, 28 mg L^{-1} K_2HPO_4, 4 mg L^{-1} $CaCl_2 \cdot 2H_2O$ and 7 mg L^{-1} NaCl which led to an initial dissolved organic carbon (DOC) of 25 mg L^{-1}. RE was a secondary treated effluent sample taken from the municipal wastewater treatment plant (MWTP) of El Ejido (province of Almería, Spain). The qualitative characteristics of the RE sample are presented elsewhere (Michael et al., 2012).

2.3. Experimental procedure

Solar Fenton experiments were performed at the PSA in a compound parabolic collector (CPC) pilot plant designed for solar photocatalytic applications. The pilot plant is operated in batch mode and is basically comprised of four modules containing 5 Pyrex glass tubes each (*i.d.* 46.4 mm, *e.d.* 50 mm) mounted on a fixed platform tilted 37° (local latitude). The overall capacity of the reactor (V_T) consists of the total irradiated volume (V_i = 44 L) and the dead reactor volume (tank, piping and valves). The maximum capacity of the plant is 82 L but in our case it was operated with 75 L. A diagram and description of this system are presented elsewhere (Lapertot et al., 2006). Solar ultraviolet radiation (UV) was measured by a global UV radiometer (Kipp & Zonen, model CUV 3) mounted on the same platform as CPCs.

At the beginning of all the photocatalytic experiments (the collectors were covered to avoid any photoreaction during preparation), the reactor was filled with the water matrix. Then, an OFX standard solution (10 mg L^{-1}; this accounts to approximately 6 mg L^{-1} of DOC) was added directly to the photoreactor, and after homogenization (15 min) a sample was taken representing the initial drug concentration ($[OFX]_0$). The recirculation of the solution in the reactor was chosen to be 15 min, a time duration sufficient for good mixing, according to the operative flow rate and the detection of the examined compound at the outlet of the system. After that, the pH was adjusted with H_2SO_4 2 N (pH = 2.8–2.9) and 2 mg L^{-1} of ferrous iron solution was added followed by mixing for 15 min before sampling. Finally the first dose of hydrogen peroxide (2.5 mg L^{-1}) was added, a sample was taken after some minutes of dark Fenton process and the collectors were uncovered. Samples were withdrawn from the reactor when the hydrogen peroxide was completely consumed and another dose was added. This procedure enabled us to obtain reliable and stable samples (no reaction in the dark and no toxic effect of any residual H_2O_2) for evaluating TPs and bioassays in short steps with low conversion between samples.

It should be noted that, an initial substrate concentration of 10 mg L^{-1} (although considerably higher than the typically found in environmental samples) was applied in order to convincingly elucidate the oxidation products. Moreover, the low concentrations of iron and peroxide were selected after testing at higher concentrations, so that TPs and toxicity would develop more slowly and these parameters could be evaluated more accurately, securing at the same time maximum transformation and OFX removal. Additionally, since all the experiments were performed in the presence of doses of hydrogen peroxide that were totally consumed before adding a subsequent dose, the illumination time cannot be considered for any discussion in the present work.

2.4. Analytical methods

OFX degradation in the treated samples was evaluated using an HPLC-DAD system (Agilent Technologies, series 1100) equipped with a C_{18} column (Phenomenex Gemini, 5 μm, 3 × 150 mm) and operated at a flow rate of 0.5 mL min^{-1}. An isocratic method, with 10% HPLC-grade acetonitrile and 90% ultrapure water acidified with 25 mM formic acid mobile phase, was employed with detection of OFX at λ = 290 nm ($t_R \approx 12$ min). The system control and the data evaluation were conducted via a PC interface with Agilent ChemStation® software. Mineralization was monitored by measuring the dissolved organic carbon (DOC) by direct injection of the filtered samples (PTFE 0.20 μm, Panreac) into a Shimadzu-5050A TOC analyzer with an NDIR detector calibrated with standard solutions of potassium phthalate. The organic acids generated during the process were separated on a Dionex DX-600 Ion Chromatograph equipped with a Dionex Ionpac AS11-HC 4 × 250 mm column. Samples were filtered using 0.22 μm syringe driven filters (Millipore) into the sample vials provided for the Dionex autosampler. Standard solutions were injected with every run to ensure the correct operation of the system. The gradient elution was performed using NaOH (1–60 mM) solution at 1.5 mL min^{-1}. Colorimetric determination of total iron concentration with 1,10-phenanthroline was performed in the treated samples following the ISO 6332 (1988). The residual H_2O_2 remaining in the treated samples taken after some minutes of dark Fenton was measured using the spectrophotometric method (Unicam-II spectrophotometer) employing ammonium metavanadate as described by Oliveira et al. (2001). The absence of H_2O_2 in the samples was also checked using the Merckoquant® test sticks.

Oasis HLB cartridges (200 mg, Waters Corporation) were used for solid phase extraction (SPE). The cartridges were conditioned with 4 mL MeOH followed by 4 mL of acidified deionized water (pH ≈ 3) at a flow rate of 1 mL min^{-1}. After the conditioning step, 40 mL of the sample was percolated through the cartridges at a flow rate of 1 mL min^{-1} followed by 3 mL of deionized water. The cartridges were then dried under vacuum for 15–20 min and final elution was performed with 2 × 2 mL of MeOH at 1 mL min^{-1}. The extracts were evaporated under a gentle nitrogen stream and reconstituted with 1 mL of methanol–water (5:95, v/v).

The TPs generated during the photocatalytic degradation of OFX in all the water matrices tested, were monitored on Q-ToF-MS (Waters) connected to a UPLC Acquity system (Waters) equipped with a reversed-phase Waters Acquity BEH C_{18} analytical column (1.7 μm; 2.1 × 50 mm). The mobile phase was acetonitrile (A) and water acidified by 0.01% formic acid (B) at a flow rate of 0.4 mL min^{-1}. The chromatographic method held the initial mobile phase composition (5% A) constant for 0.5 min, followed by a linear gradient to 95% A in 8.5 min and then maintained at 5% for 2 min. The Q-ToF-MS system was equipped with an electrospray interface operating in the positive ion mode using the experimentally measured *m/z* values of the precursor and fragment ions. Data were processed with MassLynx™ software incorporated in the instrument.

2.5. Toxicity assays

A commercial bioassay, Biofix®Lumi-10, based on inhibition of chemiluminescence emitted by the marine bacteria *Vibrio fischeri*, was performed for toxicity evaluation. Alteration in light output was measured after 15 and 30 min of exposure at 15 °C. Adjustment of the sample pH to 7 ± 0.5 was carried out prior to analysis while the osmotic pressure of the samples was adjusted with NaCl in order to obtain salinity of 2%.

Respirometry assay was also carried out using a BM-T respirometer (from Surcis SA) consisting of a 1 L capacity biological reactor with temperature control (to maintain the temperature at 20 °C by external circuit) and a Stratos 2402 Oxy oximeter. Respirometry is based on the consumption of oxygen by the microorganisms present in the activated sludge and its operation is based on closed-loop batch processing in which the dissolved oxygen contained in the sludge is continuously measured. At first, activated sludge was collected from the municipal WWTP of Almería and maintained in aeration without the addition of organic source for a day in order to remove any traces of organic substrate and to obtain the sludge in endogenous respiration phase. The supply of oxygen was continuously maintained to keep the saturation in the water. In addition, the amount of volatile suspended solids (g_{VSS} L^{-1}) present in the sludge was determined. In order to remove ammonia and therefore eliminate any possibility of nitrification, allylthiourea (ATU) was added to the sludge in the proportion of ATU 3 mg $(g_{VSS})^{-1}$ and left airing for 30 min before starting the test. The analysis was performed comparing the bacterial activity developed in two assays: (i) the reference, which consisted of 900 mL of sludge and 100 mL of distilled water with added substrate and; (ii) the mixture which consisted of 900 mL of sludge and 100 mL of sample with added substrate. The substrate was 0.5 g sodium acetate $(g_{VSS})^{-1}$ dissolved in 100 mL of distilled water. The test of the reference was extended until it reached the maximum respiration rate (R_{smax}). After obtaining the R_{smax} of the reference, the analysis was performed for each sample (mix). This test was maintained during the same or longer time than the one needed for the reference to achieve R_{smax}. If there was no toxicity, then the respiration rate of the examined sample was considered to be equal or higher than in the reference test. When $R_s \ll R_{smax}$ toxicity was expressed quantitatively through the inhibition percentage (I_s, %), determined as follows:

$$I_s(\%) = 100 \times \left(1 - \frac{R_s}{R_{smax}}\right). \quad (1)$$

3. Results and discussion

Prior to the photocatalytic treatment, direct sunlight photolysis and hydrolysis were performed as preliminary experiments, with the aim of assessing whether these effects contribute to antibiotic degradation. Hydrolysis and direct sunlight photolysis experiments were carried out in aqueous solutions of OFX at initial concentration of 10 mg L^{-1} at inherent pH (pH = 6.5). The photolytic experiments showed that after 500 min (>8 h) of solar irradiation, 72% of the initial concentration of OFX was removed; however this degradation was achieved in much longer time than the one used during the photocatalytic tests (i.e. ~20% after 4 h). The results derived from the photolytic degradation of OFX are in accordance with those reported by Park et al. (2002) and Calza et al. (2008). On the other hand, no mineralization occurred within the same experimental period possibly indicating the formation of stable oxidation products, which are more resistant to photodegradation than OFX itself. The hydrolysis experiments showed negligible degradation of the investigated compound within 360 h. Hydrolysis of OFX was not expected because this compound does not possess structural features that can be readily hydrolyzed at the temperatures relevant to environmental conditions.

3.1. Solar Fenton experiments

One important issue of the pilot scale study was to determine the effect of the water matrix composition on the solar Fenton efficiency regarding the extent of mineralization. For this purpose, the experimental protocol that was followed, involved the use of relatively simple water matrices (DW and SW), as well as matrices of increased complexity, by studying SWW and finally RE.

It is well known that inorganic species (i.e. chlorides, sulfates) significantly reduce the photo-Fenton reaction rate (Pignatello et al., 2006) due to their complexation with Fe^{2+} or Fe^{3+}, yielding iron-chloride or iron-sulfate complexes that reduce the amount of active iron, and to the scavenging of hydroxyl radicals and formation of less reactive inorganic ions (De Laat et al., 2004). Fig. 1(a) depicts the mineralization that accompanies degradation of OFX and the corresponding hydrogen peroxide requirements (in mg L^{-1}) during the solar Fenton treatment in DW and SW. As can be seen, the maximum OFX mineralization (78.1%) in DW was accomplished with 12 mg L^{-1} of H_2O_2 consumption, while at the same consumption of H_2O_2, 58.3% of DOC removal was achieved in SW. Solar Fenton was less efficient in terms of DOC reduction in SW since higher hydrogen peroxide doses were required for less mineralization. This may be associated with the presence of inorganic ions (Cl^-, SO_4^{2-}) in SW (its composition is provided in the Experimental procedure section 2.3), which may act as scavengers of the hydroxyl radicals order that may form complexes, thereby decreasing the process efficiency. Moreover, this suggests that the oxidation products formed from the degradation of OFX are slowly mineralized in SW, although their degradation is gradually accelerated with increasing peroxide consumption. However, although the mineralization rate is influenced by the presence of these anions, the solar Fenton efficiency was still sufficient with regard to the parent compound degradation. The above results indicate however, the lack of complete mineralization in both DW and SW, implying that OFX was transformed into stable organic intermediates that are resistant to further degradation by solar Fenton process.

Additional experiments were conducted in order to determine the efficiency of the solar Fenton using SWW and RE. From Fig. 1(b) it is obvious that the presence of dissolved organic matter and higher salt content in SWW and RE (they contain about 25 and 10 mg L^{-1} DOC, respectively) led to lower mineralization per dose of hydrogen peroxide compared to DW and SW (Fig. 1(a)). In the case of RE, the DOC removal achieved at 12 mg L^{-1} of peroxide consumption was 35.8% whereas in the case of SWW it was 40.5% at the same peroxide consumption. The presence of natural organic compounds occurring in the wastewater matrices can affect the degradation rate of the target compound and the mineralization since they can exhibit significant iron complexation (or can alter the redox cycling of iron) and thereby change the formation rate of hydroxyl radicals (Lindsey and Tarr, 2000). In addition, the slower mineralization rate in the wastewater samples may be attributed to the presence of dissolved organic matter (DOM), which can hinder the sunlight absorption or can act as a major scavenger by readily reacting with HO• (Westerhoff et al., 2007).

Ion chromatograms of the above treated solutions exhibited the presence of peaks related to short-chain linear carboxylic acids formed during the solar Fenton process. The analyses allowed determining four carboxylic acids i.e. formic (t_R = 11.35 min), acetic (t_R = 8.66 min), oxalic (t_R = 27.8 min) and propionic (t_R = 10.2 min) acids as the final products of OFX during the solar Fenton experiments in DW and SW. The evolution profile of the acids detected along with the concentration profile of organic carbon (coming from acids) and DOC in the case of DW is depicted in Fig. 2(a).

Acetic and formic acids occurred at the same concentration level at 7.2 mg L^{-1} peroxide consumption (acetic = 2.5 mg L^{-1}; formic = 2.1 mg L^{-1}), while oxalic and propanoic acids are accumulated in lower concentration, being completely removed at the end of the

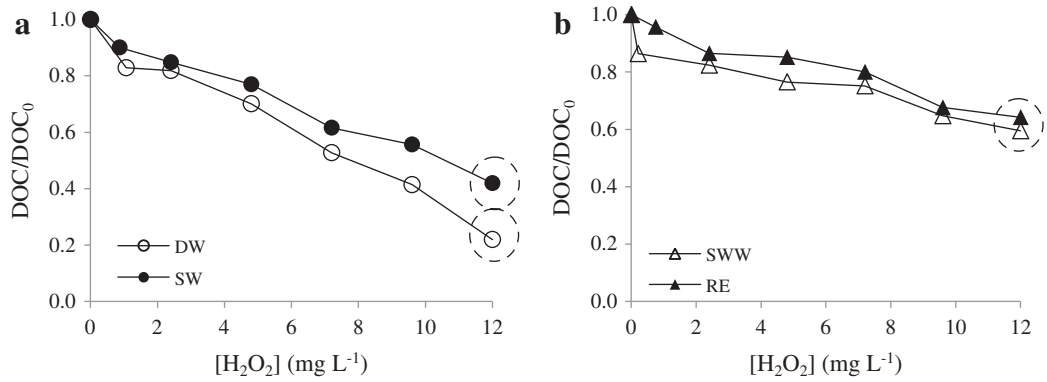

Fig. 1. OFX mineralization during solar Fenton experiments in each type of matrix: (a) DW-SW; (b) SWW-RE. Experimental conditions: $[OFX]_0 = 10$ mg L^{-1}; $[Fe^{2+}] = 2$ mg L^{-1}; $[H_2O_2] = 2.5$ mg L^{-1} (in doses); $pH_0 = 2.8$–2.9.

treatment. With the 22 mg L^{-1} H_2O_2 concentration, 17% of the remaining DOC is attributed to these acids (total carbon acids = 0.34 mg L^{-1}, DOC = 1.96 mg L^{-1}). Comparison of results in Fig. 2(a) with those in Fig. 2(b) evidences the slower formation and degradation of these acids in SW since the formation and decay of these acids required higher doses of peroxide compared to that needed in DW. The maximum concentrations of the acids generated in SW were 2.22 mg L^{-1} for acetic acid (9.6 mg L^{-1} H_2O_2) and 1.45 mg L^{-1} for formic acid (7.2 mg L^{-1} H_2O_2), while oxalic and propionic acids were present at much lower concentration level.

3.2. Characterization of major transformation products by UPLC–ESI-QToF-MS

Transformation products (TPs) generated during the pilot-scale solar Fenton treatment of OFX were elucidated and the possible influence of the water-matrix composition on the degradation pathway was assessed. In order to determine the major TPs of the investigated antibiotic in each matrix studied, samples from the solar Fenton experiments were analyzed in a full-scan mode using an UPLC–QToF-MS/MS instrument. With the objective of investigating the TPs of the examined compound, a relatively low amount of H_2O_2 (2.5 mg L^{-1} in doses) was used in the photocatalytic experiments, which enabled obtaining slow kinetics and provided favorable conditions for the determination of TPs. Structure elucidation was based on the accurate mass measures provided by the QToF analyzer which allows obtaining the elemental composition of the protonated molecule as well as of the fragment ions. The low errors obtained in all cases provided a high degree of certainty in assigning molecular composition. The analyses are accompanied by a large amount of information which is reported in Table S1 (Supplementary information). This table summarizes the experimental and calculated masses of the molecular and fragment ions, the relative mass errors, the double bond equivalents (DBEs) and the proposed elemental compositions for the TPs. The aforementioned data were obtained under optimized conditions of collision energy and cone voltage of the QToF mass spectrometer. At this point, it is worth noting that not only the relative mass errors served as a criterion in proposing the most likely elemental composition, but calculation of the corresponding double-bond equivalents (DBE) afforded a straightforward means of proposing the most likely empirical formula. It is also noted that *m/z* refers to the protonated *m/z*.

The UPLC–(+)ESI-QToF-MS product ion spectrum and putative assignment of characteristic fragment ions of the OFX molecule (*m/z* 362; $C_{18}H_{21}FN_3O_4$) are shown in Fig. S1 (Supplementary information). The collision-induced-dissociation experiments revealed the formation of several fragment ions at *m/z* 58–*m/z* 318 as shown in Table S1 (Supplementary information).

3.2.1. Proposed transformation mechanisms of OFX during solar Fenton oxidation

Along with the antibiotic degradation and the transient formation of carboxylic acids, seven TPs characterized by different *m/z* ratios were identified, as may be seen in the MS spectra recorded in Fig. S2

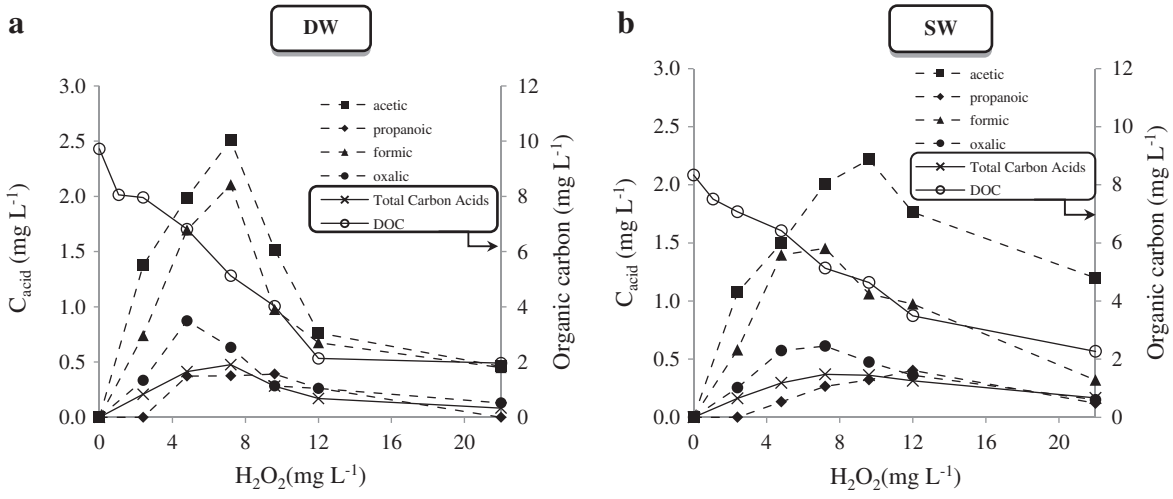

Fig. 2. Carboxylic acid formation during degradation of OFX solution (10 mg L^{-1}) with solar Fenton in: (a) DW; and (b) SW.

(Supplementary information). Chromatographic analysis allowed the identification of the same TPs during OFX degradation by solar Fenton in all the examined water matrices (DW, SW, SWW and RE except **P6** that was not detected in DW); however, some important differences in the evolution profile were observed and these are discussed further below.

The major reaction mechanisms that have been reported to occur for FQs in various media (some environmentally relevant or not; i.e. wastewater effluents, deionized water; biological samples, co-dissolved ionic species media, etc.), include heterolytic defluorination (reaction with fluoroaromatics), decarboxylation and modifications of the piperazine and quinolone moieties (Albini and Monti, 2003; De Witte et al., 2009; An et al., 2010; Paul et al., 2010). In the present study, the analyses confirm the formation of TPs through the defluorination reaction, accompanied by some degree of piperazine and quinolone substituent transformation which is in agreement with previous studies reporting the photodegradation of OFX. Decarboxylation however, was not observed at any case in the present study. Scheme 1 depicts the main TPs formed during OFX oxidation alongside the tentative phototransformation pathway.

3.2.1.1. Defluorination. The defluorination reaction resulting during the solar Fenton oxidation of OFX (6-*mono*fluoroderivative), involves the photosubstitution of the fluorine atom by a hydroxyl group (−HO) yielding the corresponding 6-hydroxyofloxacin (**P4**, *m/z* 359). Fig. S2(d) depicts the mass spectrum of **P4** indicating the net mass loss from the formed **P4**. In principle, this reaction involves either unimolecular fragmentation of the C−F bond in the excited state or water addition followed by fluorine anion loss (Van Eijk et al., 1989; Albini and Monti, 2003). The photosubstitution of the fluorine substituent by a hydroxyl group was also observed during the direct photolytic degradation of other related FQs, i.e. enrofloxacin and ciprofloxacin in Wammer et al. (2012) and Paul et al. (2010), respectively. In addition, the proposed structure is in good agreement with that obtained from photolysis experiments (Albini and Monti, 2003), which indicate substitution of the fluorine atom by a hydroxyl group as first step in the defluorination process.

3.2.1.2. Piperazinyl substituent transformation. Solar Fenton oxidation products identified in this study indicate formation of a variety of organic products wherein the heterocyclic piperazine ring was modified. Piperazinyl moiety consists of a six-membered ring containing two nitrogen heteroatoms at opposite positions in the ring. The mechanism of this class of reactions has not yet been clarified, nor is this easy in view of their low quantum yield. According to Albini and Monti (2003), possible mechanisms involve hydrogen abstraction either by some excited state (the triplet state of the fluoroquinolone or of some impurity, such as an aromatic ketone) or by hydroxyl radicals arising through the treatment process. The TPs detected, suggest that piperazine ring transformations generally proceed by partial degradation of the alkylamino side chain. **P2** (*m/z* 335, $C_{16}H_{19}FN_3O_4$) was formed after multiple reactions, leading to enhanced degradation at the piperazinyl substituent. Based on the interpretation of the fragmentation patterns and the accurate mass data as listed in Table S1, the proposed structures of the **P2** fragment at ions are compiled in Fig. S2(b). **P2**, which is 27 Da lighter than the parent compound, could be identified as a secondary amine due to the net loss of $-C_2H_2$. **P2** has been observed previously in An et al. (2010) and van Wieren et al. (2012) during the TiO_2-heterogeneous photocatalytic degradation of OFX.

In addition, as shown in Fig. S2(e), **P5** was formed during oxidation of OFX molecule at the piperazinyl substituent. Using high resolution mass spectrometry, the molecular formula for the compound **P5** with *m/z* 363 was identified as $C_{17}H_{19}FN_3O_5$ which was attributed to the net loss of $-CH_3$ and further introduction of a hydroxyl group (−HO) on the 2′ carbon of piperazinyl ring (hydroxylation). According to De Witte et al. (2008), the electron donating capacity of a methyl group compared to a hydrogen atom substituted at N4 of the piperazinyl moiety affected the formation of degradation products. An additional sequence of incorporation of an oxygen atom

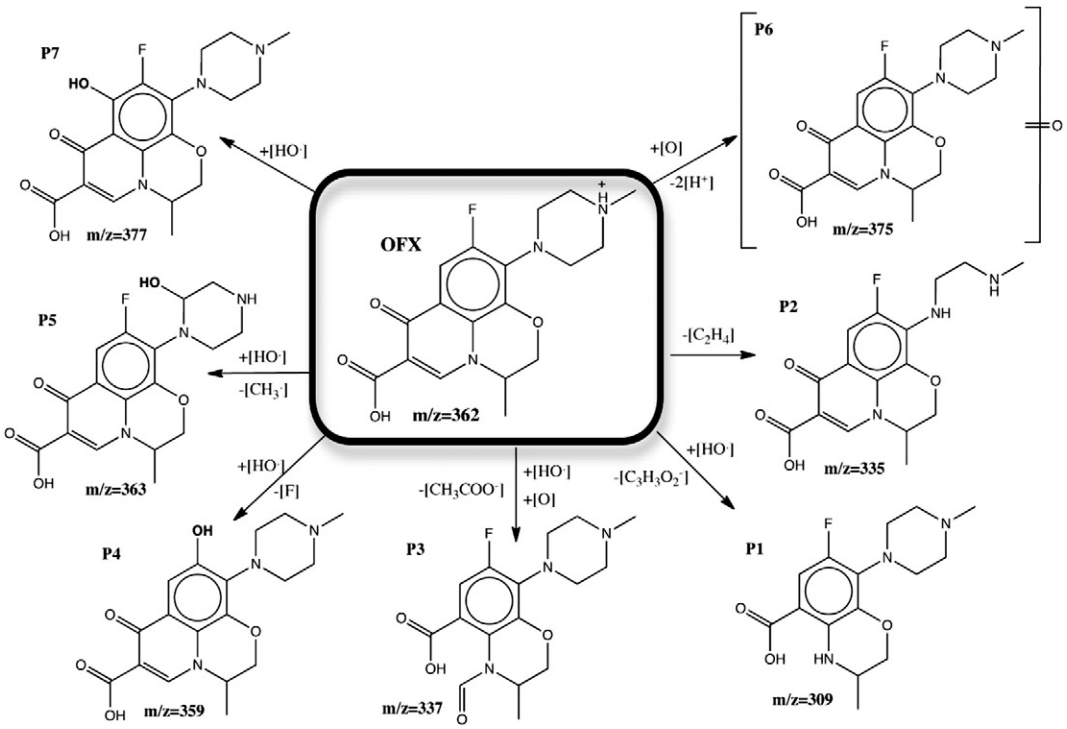

Scheme 1. Phototransformation products identified during the solar Fenton treatment of OFX in four water matrices (DW, SW, SWW and RE): Structures and *m/z* of protonated molecules.

resulted in the formation of the hydroxylketo-derivative **P6** (*m/z* 375, $C_{18}H_{19}FN_3O_5$) (Fig. S2(f)).

3.2.1.3. Quinolone moiety transformation. **P3** (*m/z* 337, $C_{16}H_{21}FN_3O_4$) indicated the transformation of the chromophore group of the molecule (loss of $-C_2$), i.e. the quinolone moiety (Fig. S2(c)). The results suggest that degradation at the quinolone moiety is mediated by HO• in agreement with previously reported ciprofloxacin degradation (De Witte et al., 2008). Based on the molecular formula and MS fragmentation, this degradation product was found to be an anthranilic acid analogue. Similar degradation products were identified during ciprofloxacin ozonation (De Witte et al., 2008). Anthranilic acid analogues were reported to occur through the direct ozonation of ciprofloxacin by Karl et al. (2006) and De Witte et al. (2008). **P1** was also formed (*m/z* 309, $C_{15}H_{21}FN_3O_3$) by the net loss of $-C_3O$ (Fig. S2(a)).

It should be noted that the heterocyclic fluorine ring remained intact during the oxidation process. Nevertheless, **P7** (*m/z* 377, $C_{18}H_{21}FN_3O_5$) was formed at the initial stages of the treatment which is attributed to monohydroxyl derivative due to the non-selectivity of the HO• attack (Fig. S2(g)).

In summary, all the TPs described above can be accounted for within the framework of the pathways shown in Scheme 1. It appears that the transformation of piperazinyl substituent was the first degradation pathway in which, the partial degradation of the heterocyclic piperazine ring was observed (**P2**, **P5**, **P6**) while the fluoroquinolone core, believed to be responsible for antibacterial activity, was unmodified. A quinolone transformation also occurred to yield **P1** and **P3**. The hydroxylation reaction with the parent compound was considered the third degradation pathway. One monohydroxyl intermediate was detected during the photocatalytic degradation of OFX (**P7**). The F atom loss due to ipso attack of the hydroxyl radical is proposed as the fourth degradation pathway (**P4**).

Regarding the AOP-mediated degradation of OFX, little attention has been paid to identifying its TPs so far, although its photochemical behavior has been widely investigated. The reaction routes proposed, although sharing certain similarities, differ from others previously reported in the literature for OFX and other related FQs with similar molecular structure as OFX.

The photo-transformation pathway of OFX using UV-photolytic and UV-heterogeneous photocatalytic treatment was recently proposed by Vasquez et al. (2012). Nine compounds were tentatively identified as TPs formed during the photolytic and photocatalytic treatments of OFX aqueous solution. According to this study, two major pathways were suggested, in which piperazinyl dealkylation and decarboxylation were considered as major transformation mechanisms. Twenty TPs were tentatively identified by UPLC–MS/MS during the sonophotocatalytic treatment of OFX spiked in secondary treated effluent (Hapeshi et al., in press). Piperazinyl dealkylation, hydroxylation, demethylation of the piperazinyl ring, decarboxylation, defluorination, cleavage of OFX molecule and oxidation of hydroxyl groups were described as major transformation mechanisms. Interestingly, none of the TPs reported in the aforementioned studies were elucidated herein, indicating that the degradation pathways and the formation of TPs depend on the type of advanced treatment applied, even though the processes are driven by the same reactive species, which is mainly HO•.

Ozonation of the quinolone antibiotic levofloxacin was investigated by De Witte et al. (2009) with focus on degradation products identification. Levofloxacin is the S-(−) form of OFX and it is an active antimicrobial agent (Okeri and Arhewoh, 2008). Nine levofloxacin ozonation products were identified indicating degradation at the piperazinyl substituent (including **P2**, **P5**) and the quinolone moiety (including **P3**). Degradation at the quinolone moiety resulted in isatin and anthranilic acid type TPs, probably formed through reaction with hydroxyl radicals.

P2 which corresponds to the partial elimination of the piperazynilic ring from levofloxacin molecule during the TiO_2-photocatalytic degradation was also proposed by An et al. (2010). An et al. (2010) reported the TiO_2-photocatalytic degradation mechanisms for three fluoroquinolones (norfloxacin, levofloxacin and lomefloxacin), including the elimination of piperazine ring, the addition of hydroxyl radical to quinolone ring, and the substitution of F atom on the aromatic ring with hydroxyl radicals.

Calza et al. (2008) studied the photocatalytic transformation of OFX and ciprofloxacin, under simulated solar irradiation using TiO_2 as photocatalyst. In the OFX molecule, the initial transformation attacks are confined to the piperazinyl moiety and to the methyl groups, while the fluoroquinolone core remained unmodified. Conversely, ciprofloxacin degradation involves two parts of the molecule: the piperazinyl moiety and the quinolone moiety.

3.2.2. Evolution profile of the main TPs in four water matrices

Although exact concentrations of the TPs cannot be determined accurately without authentic standards, a rudimentary quantification of the TPs was performed by using a comparison of their corresponding LC–MS peak areas with the peak area recorded for 10 mg L^{-1} OFX standard solution. The relative abundance of TPs against the peroxide consumption in each water matrix is depicted in Fig. 3.

The TPs described above were easily degraded in DW with their maximum intensity ratios taking place at 2.4 mg L^{-1} H_2O_2 as indicated in Fig. 3(a), and when the consumption of peroxide was equal to 7.2 mg L^{-1} all the identified TPs have been completely disappeared. It should be noted that at this peroxide consumption, the maximum concentration of the carboxylic acids was observed, while almost 30% of the DOC is abated (Fig. 1(a)). By comparing the evolution profiles for these TPs, it appears that **P3**, **P4**, **P5** and **P7** are the most abundant whereas **P1** and **P2** are the least concentrated products. **P6** was not detected in DW.

The degradation of OFX in SW exhibited different behavior compared to DW. **P3** and **P7** were the main TPs generated in SW, but, unlike in DW, they were detected in the solution until the end of the experiments (12 mg L^{-1} H_2O_2) (Fig. 3(b)). **P6** on the other hand, which was not detected in DW, appeared in the first stages of photocatalytic process in SW and disappeared at 7.2 mg L^{-1} H_2O_2. **P4** which resulted from the defluorination reaction mechanism, was detected at lower intensities compared to DW and remained until the end of the treatment. The other TPs (**P1**, **P2**, **P5** and **P7**) appeared promptly; at 2.4 mg L^{-1} H_2O_2, they reached a maximum concentration before being gradually degraded at 9.6 mg L^{-1} H_2O_2. These results indicate that differences in the transformation mechanism exist when OFX is present in SW compared with DW, probably as a consequence of the presence of Cl^- and SO_4^{2-} species in the SW matrix. These results also confirmed the lower DOC removal occurring at the end of SW experiments (58.3% at 12 mg L^{-1} H_2O_2) compared to that obtained in DW experiments.

The results demonstrate that the formation of the TPs in the matrices of increased complexity (SWW and RE) was induced with a slower rate due to the presence of the high organic and salt content present in these matrices. As previously discussed in Section 3.1, the presence of ions and organics at high concentration level in SWW and RE, inhibits the reaction with hydroxyl radicals thus, affecting the formation/degradation of the TPs. Furthermore, the presence of natural organic compounds occurring in SWW and RE can affect the degradation rate of the target compound and the formation of its TPs. These compounds (such as humic acids, fulvic acids, organic colloids) exhibit significant iron complexation (or can alter the redox cycling of iron) and thereby change the formation rate of hydroxyl radicals (Lindsey and Tarr, 2000). As can be seen in Fig. 3(c) and (d), all the TPs were detected in the treated samples at high intensities.

It is important to point out that the same TPs were identified independently of the composition of water matrix except **P6**, which was

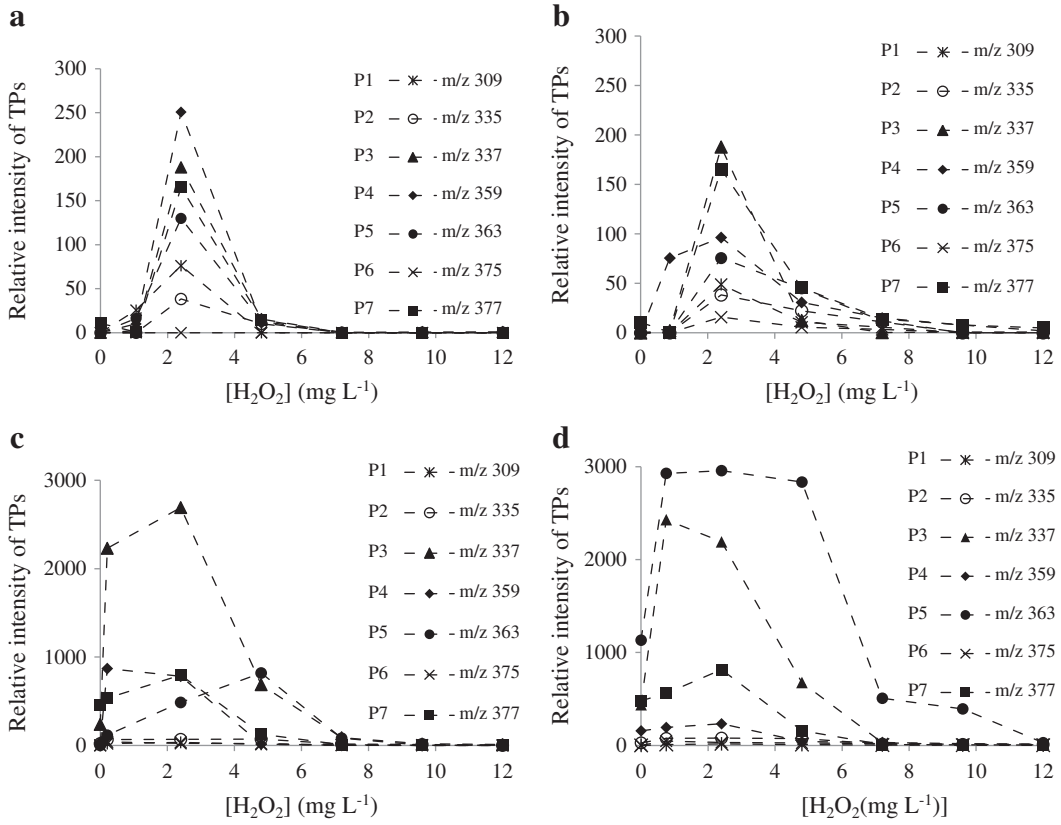

Fig. 3. Abundance of the main photo-transformation products of OFX generated during solar Fenton experiments in: (a) DW; (b) SWW; (c) SWW; and (d) RE.

not formed during the experiments in DW presumably due to the rapid reactions that took place in the solution.

3.3. Evaluation of toxicity

Considering the fact that partial mineralization took place in all the matrices tested, it was necessary to conduct toxicity measurements since more toxic compounds may be formed during the treatment process.

The toxicity assays (*V. fischeri*, respirometry) were performed in undiluted samples taken at different stages of the solar Fenton treatment using SWW and RE matrices, as it was considered more realistic than performing bioassays using DW and SW. The toxicity of OFX solution on *V. fischeri* collected at different irradiation times was measured after 15 and 30 min of incubation. Since there was no difference in inhibitory effect for the two exposure times, the data measured after 30 min of exposure are presented. The results are depicted in Fig. 4.

OFX untreated solution (RE spiked with 10 mg L^{-1} OFX, 0 mg L^{-1} H_2O_2 consumed) caused 33% inhibition of bacteria luminescence whereas a rapid increase was observed after solar Fenton process was applied. At 12.0 mg L^{-1} H_2O_2 consumption the inhibition was approximately 64%. These results demonstrate that during the evolution of solar Fenton treatment, solution toxicity increased due to the formation of oxidation products.

Interesting however, was the fact that the inhibition values observed at the OFX treated samples taken from the SWW experiments were below 7% after 30 min of exposure time (data not shown). The slight toxicity detected in the latter case, indicates that the toxic effect on bacteria in the case of RE is attributed to the compounds originally present in the RE (DOM) and the DOM by-products formed during the photocatalytic treatment rather than the substrate oxidation products. Respirometric test was also performed in the same samples and the results showed similar behavior with those obtained by the *V. fischeri* toxicity test in each matrix.

In general, the final treated samples are characterized by higher toxicity compared to the initial indicating that the oxidation products formed were moderately toxic for the organism tested. A similar behavior for the *V. fischeri* test was observed in a study of Klamerth et al. (2010). The authors suggested that the increase in bacteria inhibition during photo-Fenton treatment in RE is attributed mainly to the generation of other intermediates formed during the oxidation of organics contained in the RE matrix. In another study, the chronic growth inhibition to *V. fischeri* of OFX treated samples after UV/TiO_2 photocatalysis was investigated. A significant decrease of the *V. fischeri* growth inhibition effect was observed after 8 min of irradiation time (27 ± 6% of inhibition). A further increase in irradiation to 16 min, did not lead to any significant reduction in the inhibition indicating that the formed TPs were not toxic to *V. fischeri* (Vasquez et al., 2012).

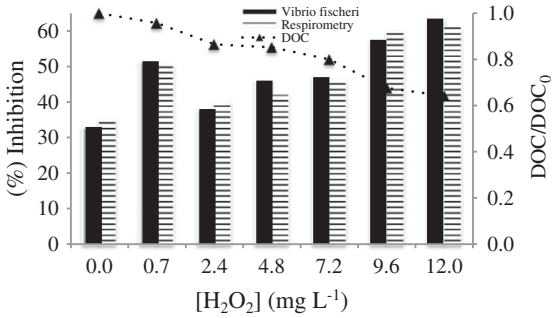

Fig. 4. (%) Inhibition of *V. fischeri* after 30 min of exposure and inhibition of bacterial activity in activated sludge during the respirometry test for samples taken during the solar Fenton process in RE.

4. Conclusions

Solar Fenton was demonstrated to be an efficient treatment for OFX degradation. However, DOC removal was found to be dependent on the chemical composition of the water matrix. The presence of salts in SW affected the mineralization rate, suggesting that hydroxyl radicals generated during the advanced treatment, were scavenged by the inorganic ions present in the solution. On the other hand, DOC removal per dose of hydrogen peroxide was lower in the case of SWW and RE due to the presence of dissolved organic matter and higher salt content in these matrices that may inhibit the reactions with the hydroxyl radicals.

The results indicated that the toxicity originates from the DOM present in RE and its oxidation products (DOM by-products) formed during the photocatalytic treatment and not from the TPs derived from the oxidation of OFX.

The transformation of OFX proceeded through the formation of seven TPs in all the water matrices. Investigations on the TPs suggest that the photocatalytic treatment was proceeding through a defluorination reaction, accompanied by some degree of piperazine and quinolone substituent transformation while a hydroxylation mechanism occurred by attack of the photocatalytically generated hydroxyl radicals. The formation profile of TPs in the more complex matrices (SWW and RE) exhibited different behavior compared to DW and SW indicating the adverse effect of the high organic and salt content present in the SWW and RE matrices in the degradation pathway.

Acknowledgments

The experimental work was funded by the European Commission under SFERA program (Solar Facilities for the European Research Area). This work was also co-funded by the Republic of Cyprus and the European Regional Development Fund through grant UPGRADING/DURABLE/0308/07 (Project title: IX-Aqua). “NIREAS” International Water Research Center (NEA IPODOMI/STRATH II/0308/09) is co-funded by the Republic of Cyprus and the European Regional Development Fund.

Appendix A. Supplementary data

Supplementary data to this article can be found online at http://dx.doi.org/10.1016/j.scitotenv.2013.04.054.

References

Akiyama T, Savin MC. Populations of antibiotic-resistant coliform bacteria change rapidly in a wastewater effluent dominated stream. Sci Total Environ 2010;408:6192–201.
Albini A, Monti S. Photophysics and photochemistry of fluoroquinolones. Chem Soc Rev 2003;32:238–50.
An T, Yang H, Song W, Li G, Luo H, Cooper WJ. Mechanistic considerations for the advanced oxidation treatment of fluoroquinolone pharmaceutical compounds using TiO_2 heterogeneous catalysis. J Phys Chem A 2010;114:2569–75.
Ash R, Mauck B, Morgan M. Antibiotic resistance of Gram-negative bacteria in rivers, United States. Emerg Infect Dis 2002;8:713–6.
Buda F, Ensing B, Gribnau MCM, Baerends EJ. DFT study of the active intermediate in the Fenton reaction. Chem Eur J 2001;7(13):2775–83.
Calza P, Medana C, Carbone F, Giancotti V, Baiocchi C. Characterization of intermediate compounds formed upon photoinduced degradation of quinolones by high-performance liquid chromatography/high-resolution multiple-stage mass spectrometry. Rapid Commun Mass Spectrom 2008;22:1533–52.
Castiglioni S, Pomati F, Miller K, Burns BP, Zuccato E, Calamari D, et al. Novel homologs of the multiple resistance regulator marA in antibiotic-contaminated environments. Water Res 2008;42:4271–80.
Clesceri LS, Greenberg AE, Eaton AD. Standard methods for the examination of water and wastewater. 20th ed. Baltimore, Maryland: American Public Health Association, American Water Works Association, Water Environment Federation; 1998.
De Laat J, Le GT, Legube B. A comparative study of the effects of chloride, sulfate and nitrate ions on the rates of decomposition of H_2O_2 and organic compounds by Fe(II)/H_2O_2 and Fe(III)/H_2O_2. Chemosphere 2004;55:715–23.
De Witte B, Dewulf J, Demeestere K, Van de Vyvere V, De Wispelaere P, Van Langenhove H. Ozonation of ciprofloxacin in water: HRMS identification of reaction products and pathways. Environ Sci Technol 2008;42:4889–95.
De Witte B, Van Langenhove H, Hemelsoet K, Demeestere K, De Wispelaere P, Van Speybroeck V, et al. Levofloxacin ozonation in water: rate determining process parameters and reaction pathway elucidation. Chemosphere 2009;76:683–9.
Fatta-Kassinos D, Hapeshi E, Achilleos A, Meric S, Gros M, Petrovic M, et al. Existence of pharmaceutical compounds in tertiary treated urban wastewater that is utilized for reuse applications. Water Resour Manag 2010;25:1183–93.
Fatta-Kassinos D, Meric S, Nikolaou A. Pharmaceutical residues in environmental waters and wastewater: current state of knowledge and future research. Anal Bioanal Chem 2011;399:251–75.
Guardabassi L, Wong DMA, Dalsgaard A. The effects of tertiary wastewater treatment on the prevalence of antimicrobial resistant bacteria. Water Res 2002;36:1955–64.
Hapeshi E, Fotiou I, Fatta-Kassinos D. Sonophotocatalytic treatment of ofloxacin in secondary treated effluent and elucidation of its transformation products. Chem Eng J 2012. http://dx.doi.org/10.1016/j.cej.2012.11.048, [in press].
ISO 6332. Water quality-determination of iron-spectrometric method using 1,10-phenanthroline; 1988.
Jeong J, Song W, Cooper WJ, Jung J, Greaves J. Degradation of tetracycline antibiotics: mechanisms and kinetic studies for advanced oxidation/reduction processes. Chemosphere 2010;78:533–40.
Karl W, Schneider J, Wetzstein HG. Outlines of an exploding network of metabolites generated from the fluoroquinolone enrofloxacin by the brown rot fungus *Gloeophyllum striatum*. Appl Microbiol Biotechnol 2006;71:101–13.
Klamerth N, Miranda N, Malato S, Agüera A, Fernández-Alba AR, Maldonado MI, et al. Degradation of emerging contaminants at low concentrations in MWTPs effluents with mild solar Fenton and TiO_2. Catal Today 2009;144:124–30.
Klamerth N, Rizzo L, Malato S, Maldonado MI, Agüera A, Fernández-Alba AR. Degradation of fifteen emerging contaminants at μg L^{-1} initial concentrations by mild solar Fenton in MWTP effluents. Water Res 2010;44:545–54.
Kümmerer K, Al-Ahmad A, Mersch-Sundermann V. Biodegradability of some antibiotics, elimination of the genotoxicity and affection of wastewater bacteria in a simple test. Chemosphere 2000;40:701–10.
Langdon KA, Warne MSTJ, Kookanaz RS. Aquatic hazard assessment for pharmaceuticals, personal care products, and endocrine-disrupting compounds from biosolids-amended land. Integr Environ Assess Manag 2010;6:663–76.
Lapertot M, Pulgarín C, Fernández-Ibáñez P, Maldonado MI, Pérez-Estrada L, Oller I, et al. Enhancing biodegradability of priority substances (pesticides) by solar Fenton. Water Res 2006;40:1086–94.
Le-Minh N, Khan SJ, Drewes JE, Stuetz RM. Fate of antibiotics during municipal water recycling treatment processes. Water Res 2010;44:4295–323.
Lhiaubet-Vallet V, Bosca F, Miranda MA. Photosensitized DNA damage: the case of fluoroquinolones. Photochem Photobiol 2009;85:861–8.
Lin AYC, Yu TH, Lateef SK. Removal of pharmaceuticals in secondary wastewater treatment processes in Taiwan. J Hazard Mater 2009;167:1163–9.
Lindsey ME, Tarr MA. Inhibition of hydroxyl radical reaction with aromatics by dissolved natural organic matter. Environ Sci Technol 2000;34:444–9.
Malato S, Fernández-Ibáñez P, Maldonado MI, Blanco J, Gernjak W. Decontamination and disinfection of water by solar photocatalysis: recent overview and trends. Catal Today 2009;147:1-59.
Mendez-Arriaga F, Esplugas S, Gime J. Degradation of the emerging contaminant ibuprofen in water by photo-Fenton. Water Res 2010;44:589–95.
Miao XS, Bishay F, Chen M, Metcalfe CD. Occurrence of antimicrobials in the final effluents of wastewater treatment plants in Canada. Environ Sci Technol 2004;38(13):3533–41.
Michael I, Hapeshi E, Michael C, Fatta-Kassinos D. Solar Fenton and solar TiO_2 catalytic treatment of ofloxacin in secondary treated effluents: evaluation of operational and kinetic parameters. Water Res 2010;44:5450–62.
Michael I, Rizzo L, McArdell CS, Manaia CM, Merlin C, Schwartz T, et al. Urban wastewater treatment plants as hotspots for the release of antibiotics in the environment. A review, Water Res 2013;47(3):957–95.
Michael I, Hapeshi E, Osorio V, Pèrez S, Petrovic M, Zapata A, et al. Solar photocatalytic treatment of trimethoprim in four environmental matrices at a pilot scale: transformation products and ecotoxicity evaluation. Sci Total Environ 2012b;430:167–73.
Novo A, Manaia CM. Factors influencing antibiotic resistance burden in municipal wastewater treatment plants. Appl Microbiol Biotechnol 2010;87:1157–66.
Okeri HA, Arhewoh IM. Analytical profile of the fluoroquinolone antibacterials. I. Ofloxacin. Afr J Biotechnol 2008;7(6):670–80.
Oliveira MC, Nogueira RFP, Neto JAG, Jardim WF, Rohwedder JJR. Quim Nova 2001;24:188.
Park HR, Kim TH, Bark KM. Physicochemical properties of quinolone antibiotics in various environments. Eur J Med Chem 2002;37:443–60.
Paul T, Miller PL, Strathmann TJ. Visible-light-mediated TiO_2 photocatalysis of fluoroquinolone antibacterial agents. Environ Sci Technol 2007;41:4720–7.
Paul T, Dodd MC, Strathmann TJ. Photolytic and photocatalytic decomposition of aqueous ciprofloxacin: transformation products and residual antibacterial activity. Water Res 2010;44:3121–32.
Pignatello JJ, Oliveros E, MacKay A. Advanced oxidation processes for organic contaminant destruction based on the Fenton reaction and related chemistry. Crit Rev Environ Sci Technol 2006;36:1-84.
Rosal R, Rodríguez A, Perdigón-Melón JA, Petre A, García-Calvo E, Gómez MJ, et al. Occurrence of emerging pollutants in urban wastewater and their removal through biological treatment followed by ozonation. Water Res 2010;44:578–88.
Santoke H, Song W, Cooper WJ, Greaves J, Miller GE. Free-radical-induced oxidative and reductive degradation of fluoroquinolone pharmaceuticals: kinetic studies and degradation mechanism. J Phys Chem A 2009;113:7846–51.
Schwartz T, Kohnen W, Jansen B, Obst U. Detection of antibiotic-resistance genes in wastewater, surface water and drinking water biofilms. FEMS Microbiol Ecol 2003;43:325–35.

Sirtori C, Aguera A, Gernjak W, Malato S. Effect of water-matrix composition on trimethoprim solar photodegradation kinetics and pathways. Water Res 2010;44(9):2735–44.
Van Eijk AMJ, Huizer AM, Varma CAGO, Marquet J. Am Chem Soc 1989;111:88.
Van Wieren EM, Seymour MD, Peterson JW. Interaction of the fluoroquinolone antibiotic, ofloxacin, with titanium oxide nanoparticles in water: adsorption and breakdown. Sci Total Environ 2012;441:1–9.
Vasquez MI, Garcia-Käufer M, Hapeshi E, Menz J, Kostarelos K, Fatta-Kassinos D, Kümmerer K. Chronic ecotoxic effects to Pseudomonas putida and Vibrio fischeri, and cytostatic and genotoxic effects to the hepatoma cell line (HepG2) of ofloxacin photo(cata)lytically treated solutions. Science of the Total Environment 2013;450–451:356–65.
Wammer KH, Korte AR, Lundeen RA, Sundberg JE, McNeill K, Arnold WA. Direct photochemistry of three fluoroquinolone 1 antibacterials: norfloxacin, ofloxacin, and enrofloxacin. Water Res. 2013;47:439–48.
Westerhoff P, Mezyk SP, Cooper WJ, Minakata D. Electron pulse radiolysis determination of hydroxyl radical rate constants with Suwannee River fulvic acid and other dissolved organic matter isolates. Environ Sci Technol 2007;41:4640–6.
Zuccato E, Castiglioni S, Bagnati R, Melis M, Fanelli R. Source, occurrence and fate of antibiotics in the Italian aquatic environment. J Hazard Mater 2010;179:1042–8.